Renewable Energy 92 (2016) 366–375

Contents lists available at ScienceDirect

Renewable Energy

journal homepage: www.elsevier.com/locate/renene

Fast optimisation of tidal stream turbine positions for power generation in small arrays with low blockage based on superposition of self-similar far-wake velocity deficit profiles

Peter Stansby*, Tim Stallard

School of Mechanical, Aerospace and Civil Engineering, University of Manchester, Manchester M13 9PL, UK

ARTICLE INFO

Article history:
Received 23 October 2015
Received in revised form
1 February 2016
Accepted 7 February 2016
Available online 19 February 2016

Keywords:
Tidal stream turbine
Array
Velocity deficit
Superposition
Blockage
Optimisation

ABSTRACT

Far wake velocities of a single horizontal axis three-bladed turbine in shallow flow have been measured previously in the laboratory and shown to have self-similar velocity deficit profiles. Wake velocities of arrays of turbines with one, two and three transverse rows have also been measured and simply superimposing the velocity deficits for a single turbine is shown to give accurate prediction of combined wake width and velocity deficit, accounting for variable downstream blockage through volume flux conservation. Array efficiency is defined as the ratio of total power generated to what would be generated by the same turbines in isolation. From prescribed initial turbine positions, generally determined intuitively or by practical considerations, adjusting the turbine positions to increase the power from each turbine, using the chain rule, shows that relatively small movements of 3–4 rotor diameters may increase array efficiency to over 90%.

1. Introduction

Several prototype tidal stream turbines have been developed and deployed individually showing good performance. The next stage is to deploy as arrays for significant energy capture and at least two sites are planned for deployment within the next decade. Array interaction effects due to wake velocity deficits that reduce power of downstream turbines are clearly important particularly since power for a given power coefficient is proportional to velocity cubed. Models of flow in arrays have been based simply on the idea that a turbine thrust in a shallow water depth-averaged model may be imposed to simulate wake characteristics, e.g. Refs. [3,5,13]. However comparison with experimental data for a fence of turbines close to a headland has been shown to underestimate velocity deficit [4]. This has been supported through some investigations in parallel channel flow by the authors (unpublished) using the depth-averaged model of [18]. With an axial induction factor adjusted to give the correct thrust for a particular mesh, wake velocity deficits were considerably underestimated compared with experiments presented herein. Artificially increasing thrust coefficient could improve the wake velocity locally but the downstream variation was not correct and wakes widths were invariably too narrow. This approach had previously also been applied to arrays of pile groups where it was shown that large-scale wake features may be reproduced by increasing drag coefficients from their physical values [2]. Ref. [5] optimised power generation from arrays by moving turbine positions using a gradient based algorithm with the adjoint approach.

Wake interaction effects may also be investigated using computational fluid dynamics (CFD). Blade element momentum (BEM) methods coupled with Reynolds averaged Navier Stokes (RANS) models provide a computationally tractable approach for small turbine arrays. Ref. [8] used this approach for up to 14 turbines with some manual optimisation based on observations for improving power generation from three-turbine arrays. This RANS BEM approach has since been compared with experiment for array configurations presented in this paper [10].

Here we are concerned with general arrays with low blockage and low Froude number. Free surface effects will be minimal. Experimental measurements of wake velocity are available for a single turbine and arrays with one, two and three rows. The velocity deficit in the far wake of a single turbine shows two-dimensional self-similar characteristics [15]. For multiple rows

* Corresponding author.
E-mail address: p.k.stansby@manchester.ac.uk (P. Stansby).

http://dx.doi.org/10.1016/j.renene.2016.02.019

wake velocities will be compared with those obtained by superimposing the velocity deficit of a single turbine to account for the velocity reduction of one turbine in the wake of another. This approach has been applied to the self-similar flow fields of wind turbine wakes [6]. Recently [7] compared this approach with three others for flow through an array of two turbines computed using LES (large eddy simulation) and showed it gave better predictions than wake merging methods which have also been applied to tidal stream turbine arrays, neglecting blockage [11]. Using the velocity deficit superposition approach, positions of turbines will be moved from prescribed initial positions to increase individual power generation and hence total power using an algorithm based on the chain rule.

2. Experimental arrangement

The experimental arrangement has been described previously for studies of the flow downstream of a single horizontal axis three-bladed rotor, a transverse row of these rotors and the arrays of this study in shallow turbulent flow [10,14,15] respectively. This is summarised here. Velocity measurements were made with Nortek ADVs, forces with a strain-gauged load balance and power from torque supplied by a DC motor (with friction subtracted) times the rotation speed measured by a digital encoder; details are reported in Refs. [14,15]. The rotors had diameter $D = 0.27$ m in a channel of width $w = 18.5D$ (5 m) and depth $h = 1.67\ D$ (0.45 m). The average flow velocity was 0.46 m/s. For each array configuration a central upstream turbine axis was located $22D$ from the inflow, at mid-span and at mid-depth. The foil sections were selected for high lift to drag ratio at a chord Reynolds number of approximately 3×10^4 (typical at three-quarter radius at a tip speed ratio of 4.5) and with radial variation of pitch angle and chord length selected to represent the operating point of a full-scale rotor [19]. Streamwise thrust, applied torque and rotational speed of each rotor were sampled at 200 Hz for each rotor. Measured force is reduced by the drag measured on the supporting tower to give thrust. Measurement of the mean flow and turbulence characteristics taken at the plane of the upstream row indicate that the vertical profile of mean velocity follows the log law. Depth average turbulence intensity is 12% in the streamwise direction and 9% in the vertical and lateral directions. The integral length scales of the ambient turbulence measured by a two point cross correlation method at mid-depth are $0.56h$, $0.33h$ and $0.25h$ in the streamwise, transverse and vertical axes respectively. Sample duration was 900 s for these measurements. Length-scales were also estimated by an auto-correlation method providing similar values at mid-depth. It is well known that horizontal scales are greater than vertical in shallow flows and these scales are of similar magnitude to field measurements, e.g. Ref. [12]. Experimental measurements for this paper were obtained for rotors arranged in six different array configurations with three to twelve turbines. For each rotor constant retarding torque was applied by the dynamometer system and defined to develop a tip-speed-ratio of 4.5 when in isolation. For each array a number of wake traverses were obtained at planes downstream of the final row of the array. These included vertical profiles directly downstream of each rotor and transverse profiles at hub-height. Each wake traverse comprised samples of 60 s duration sampled at 200 Hz. During each wake traverse, streamwise force, torque and rotational speed for each rotor were recorded.

3. Self-similar velocity deficit superposition and blockage

For the wake of the single turbine of this study the velocity deficit has been shown to become two-dimensional and self-similar for distances greater than 8 diameters downstream [15]. At maximum power coefficient C_P with $\beta = 4.5$ the equations for centreline velocity deficit ΔU_{max} and wake half width y_{half} at downstream distance x are given by

$$\frac{\Delta U_{max}}{U_0} = -0.126 + 0.8639\Big/\sqrt{x/D} \tag{1}$$

$$\frac{y_{half}}{R} = 0.5 + 0.4118\ \sqrt{x/D} \tag{2}$$

with the transverse deficit $\Delta U(y)$, where y is distance from centreline, given by

$$\frac{\Delta U(y)}{\Delta U_{max}} = exp\left(-\ln(2)\frac{y^2}{y_{half}^2} \right) \tag{3}$$

These formulae have also been shown to give remarkably accurate prediction of depth-averaged velocity deficit extended to distances between $4D$ and $8D$ downstream. The torque in the array was controlled to give the constant value associated with maximum power coefficient C_P at $\beta = 4.5$ for ambient flow conditions, giving $C_T = 0.89$. The β values for downstream turbines defined relative to the ambient flow varied in the range of about 4–6. The corresponding thrust coefficient of downstream turbines varied in the range 0.74–0.9; this is the dominant factor in determining wake characteristics and the same velocity deficit formulae are assumed to apply.

To implement wake superposition first the velocity deficits of upstream turbines are imposed on the flow field, represented on a Cartesian mesh. The velocity at downstream turbines will be reduced if within the wake of an upstream turbine thus defining a new onset velocity. This velocity may be interpreted as the average over the disc area but this is within 1% of the hub velocity for the cases studied. The velocity deficits of these downstream turbines are then superimposed on the flow field. In addition blockage needs to be considered for comparison with experiment in a confined channel. We consider three rows (row 1 upstream to row 3 downstream). First assume that the onset velocity U_0 applies at row 1 with upstream volume flux q_0. This gives the downstream flux q_1 at row 2 with superposition of the velocity deficits from row 1 turbines. q_1 will be less than q_0 and this is corrected by a blockage correction factor q_0/q_1 so that the velocity onset on the turbines is $U_0\ q_0/q_1$. The velocity field downstream of row 1 is thus defined by this velocity with superimposed velocity deficits and stored on a mesh. This provides a first approximation for the onset flow for row 2 and with superimposed velocity deficits velocities at row 3 are defined giving a flux q_2 at row 3. q_2 is less than q_0 and the velocity onset on row 2 is multiplied by a blockage correction factor q_0/q_2 to give the correct flux at row 3. The velocity field downstream of row 2 is thus modified and the velocities stored on the mesh updated. This now provides the first approximation for the onset flow for row 3 and with superimposed velocity deficits velocities downstream (either $4D$ or $8D$ here) are defined giving a flux q_3. Again this will be less that q_0 and the velocity onset on row 3 is multiplied by a blockage correction factor q_0/q_3 to give the correct flux. Further rows may be incorporated in the same way but are not considered here.

This is for one flow direction and the flow field is steady. In tidal flows the flow reverses and the wake interaction process is applied over rows in the reverse order. In the code velocity direction is defined by the angle of incidence so variable angle onset flow may be taken into account although only values of 0 and 180^0 are investigated here. This does imply that the residual wake from one half cycle has no effect in the following half cycle.

Experimental results for 6 array configurations in uni-

directional flow are compared here: one transverse row of 3, one of 5, two rows of 5 with in line turbines at 8D spacing, two rows of 3 and 4 turbines staggered at 4D and 8D spacing and three rows of 3,4 and 5 turbines staggered at 4D spacing. The transverse spacing was 1.5D for all cases. For these arrays blockage is significant as listed in Table 1 with blockage correction factors. The conventional 'wind tunnel' approach is to estimate increase in dynamic pressure through an empirical formula [9] in order to correct pressures and forces on a body. The correction is different for axisymmetric and two-dimensional bodies and has been investigated in two dimensions by Ref. [16] showing good prediction of vortex shedding wake frequency. The ratio of increase in velocity to onset velocity is half the ratio of dynamic pressure increase to the onset value. This may be compared with the results for a single row based on the method described above given in Table 1. The Maskell values are given by $1/2cBC_D$ where B is blockage area ratio, C_D is drag coefficient equivalent to thrust coefficient C_T and $c = 1$ for two-dimensional bodies and 2.5 for axisymmetric bodies. The values in Table 1 are given approximately by $c = 1.75$ which is consistent with axisymmetric wakes becoming two dimensional.

From Table 1 and it can be seen that the correction factor for the second row is much smaller than for the first and for the third is smaller than for the second. In order to ensure zero normal velocity on the flume side walls, velocity deficits from images of turbines in those walls may be added. However this had no discernible effect on the results.

Comparisons of downstream velocity profiles with the superposition method with these blockage correction factors are shown in Figs. 1–6 where U_x is the depth-averaged longitudinal velocity. Some features are immediately obvious. The wake width is always well predicted although in Fig. 3 for the case of two in-line rows of 5 turbines one side of the wake is slightly removed from the superposition prediction suggesting some flow asymmetry in the experiments. The transverse velocity variation at 4D downstream is less pronounced in the superposition model than in the experiments, i.e. the wakes have merged more, while there is little velocity variation at 8D in both cases. The average velocity deficit is well predicted for the cases with one row (Figs. 1 and 2) and two rows (Figs. 3–5). For the 3 row array on the other hand, the velocity deficit shown in Fig. 6 is somewhat overestimated indicating greater entrainment into the large scale wake in the experiments. The rms errors in velocity deficit are shown in Table 2. It should be mentioned that the predictions using the RANS BEM with blockage modelled directly showed similar levels of error [10]. Clearly the physics of wake interaction is complex with different turbulence length scales in the onset flow with vertical, transverse and longitudinal scales typically in the ratio 1:3:5 and wake length scales proportional to wake width. From the point of view of optimisation of individual turbine power however the most important factor is whether a downstream turbine is within the wake of an upstream turbine and this appears to be well predicted in all cases. For practical problems of tidal farms in open coastal domains blockage may not be a significant concern.

4. Optimisation method

The aim of optimisation here is to move turbine positions to increase individual power generation to take advantage of available capacity and thus increase overall energy capture from the farm. It is recognised that proposed configurations would also be based on practical considerations, ground conditions, grid connections etc. as well as locations with high current speed. The change in net power P may be defined by the chain rule where P_i , $i = 1, N$, is the individual power for each of the N turbines:

$$dP = \frac{\partial P_1}{\partial x} dx_1 + \frac{\partial P_1}{\partial y} dy_1 + \ldots\ldots\ldots\ldots + \frac{\partial P_N}{\partial x} dx_N + \frac{\partial P_N}{\partial y} dy_N \quad (4)$$

This assumes no cross coupling between turbines (without second order derivatives) which will be shown to be adequate for optimising net power although in some instances individual power may decrease slightly. It is thus necessary to determine $\partial P_i/\partial x$ and $\partial P_i/\partial y$ and this is done numerically. Each turbine is moved a small distance dx to give a new power and hence $\partial P_i/\partial x$ and then dy to give $\partial P_i/\partial y$. $dx = dy = 0.01D$ is generally used. Positions are then all changed by:

$$dx_i = \alpha \frac{\partial P_i}{\partial x}; dy_i = \alpha \frac{\partial P_i}{\partial y}; i = 1, N \quad (5)$$

where α is a constant; 0.05 was generally used. The code, written in Fortran, is quite fast requiring minutes on a laptop and little attempt was made to speed this up. The power for an individual turbine with area $A = \pi D^2/4$ in uniform flow of velocity U_0 is given by

$$P_i = \frac{1}{2} C_P \rho U_0^3 A \quad (6)$$

U_0 may be assumed to be the hub velocity in arrays or may be calculated as an integrated effect due to variation of velocity $U_x(y)$ such that

$$P_i = \frac{1}{2} C_P \rho \int_0^{\pi} 2R^2 sin^2(\theta) U_x(y)^3 d\theta \quad (7)$$

where $R = D/2$ is rotor radius, $y = y_0 + R\cos(\theta)$ and y_0 is position of the hub (rotor centre) but this made only a small difference to the optimised turbine positions and powers. The net power $P = \sum_{i=1}^{N} P_i$ is an important output. For this exercise it is assumed that each turbine is controlled to give local β for maximum C_P which is thus constant as is C_T. Note this is different from the experimental arrangement.

5. Optimisation results

Tidal flows are oscillatory and not generally completely rectilinear. However we first consider optimisation for flow in one

Table 1
Blockage corrections.

Case	Configuration	Blockage ratio	Blockage correction for each row
1	1 row of 3	0.074	1.055
2	1 row of 5	0.124	1.083
3	2 rows of 5, in line, 8D apart	0.124	1.083, 1.017
4	2 rows of 3 and 4, staggered, 4D apart	0.153	1.055, 1.012
5	2 rows of 3 and 4, staggered, 8D apart	0.153	1.055, 1.019
6	3 rows of 3,4,5, staggered, 4D apart	0.195	1.055, 1.012, 1.008

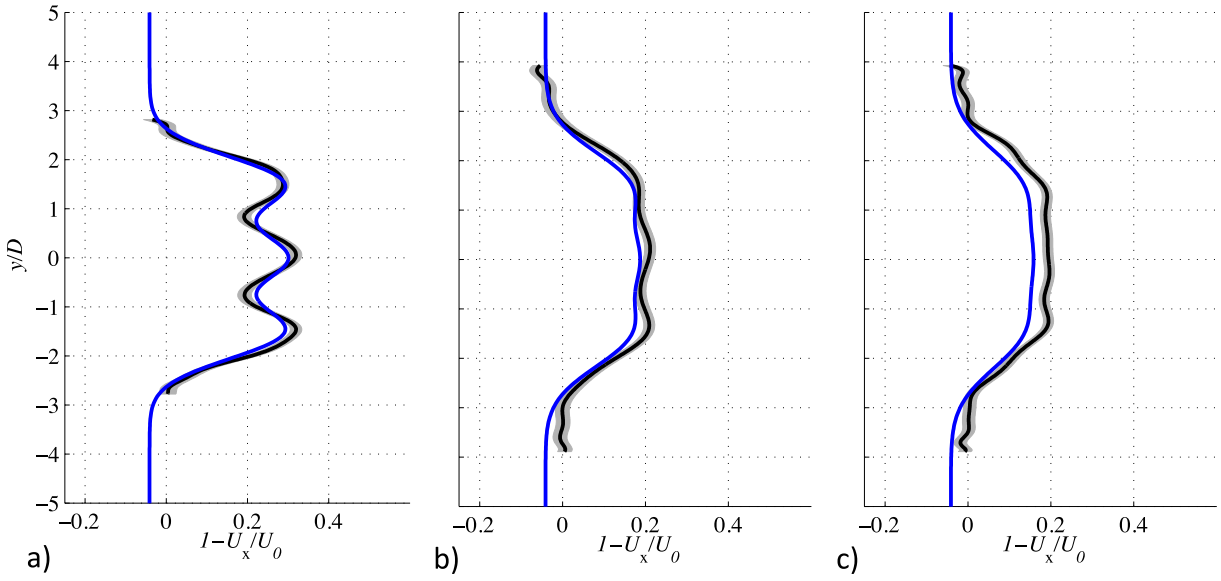

Fig. 1. Transverse velocity deficits at a) 4D, b) 8D, and c) 10D downstream for one row of 3 turbines with 1.5D transverse spacing. Superposition model (blue), experiment (black with grey showing variation). (For interpretation of the references to color in this figure legend, the reader is referred to the web version of this article.)

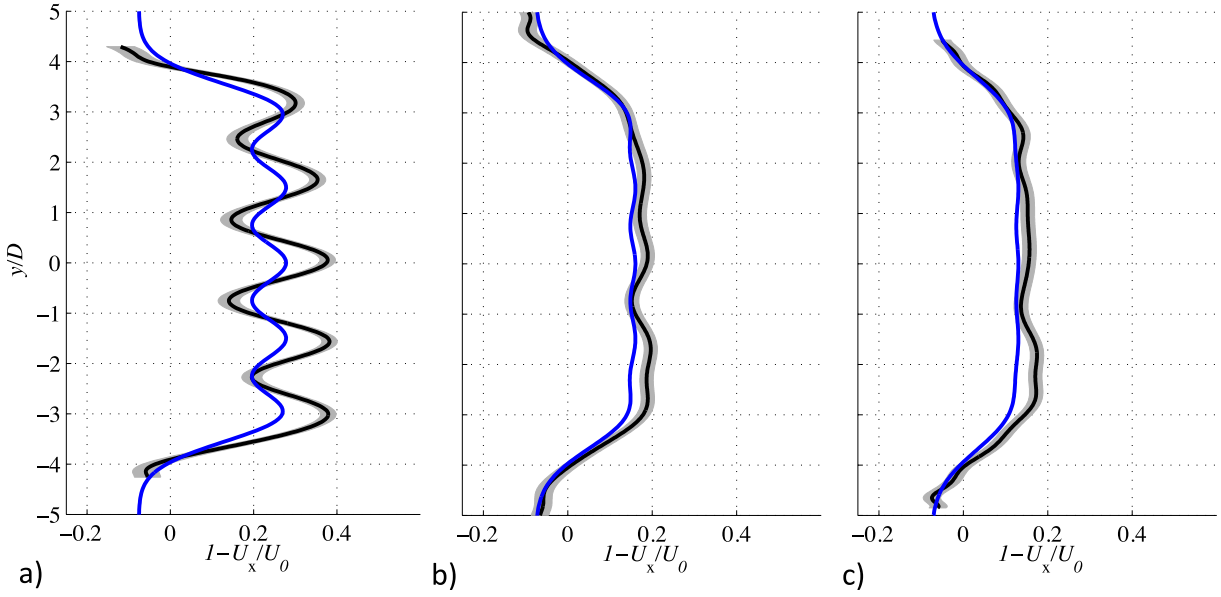

Fig. 2. Transverse velocity deficits at a) 4D, b) 8D, and c) 10D downstream for one row of 5 turbines with 1.5D transverse spacing. Superposition model (blue), experiment (black with grey showing variation). (For interpretation of the references to color in this figure legend, the reader is referred to the web version of this article.)

direction and then bi-directional rectilinear flow. Blockage is assumed to be zero. We define array efficiency as the net power divided by the sum of powers from each turbine in isolation; turbine efficiency is the individual power divided by that in isolation. For the single row or fence there is no wake effect as each turbine sees the ambient onset flow velocity. We consider the configurations investigated experimentally as initial conditions.

Figs. 7–10 show results for uni-directional flow for the 2 and 3 row configurations. The upstream turbines are not affected and the downstream turbines move causing the net power to increase with each iteration. Note that if the net power were the optimisation criterion the upstream turbines would move also but that is not considered here since in bi-directional flow upstream becomes downstream as the flow reverses and positions are correspondingly optimised. These uni-directional flows may be considered as reference cases. For the cases with two rows of 5 turbines in line at initial 8*D* spacing (Fig. 7) and of 3 and 4 turbines staggered at 4*D* spacing (Fig. 8) the net power is increased by about 14% as the outer downstream turbines move outwards and the inner turbines move downstream with a maximum distance of about 2*D*. However the case with two rows of 3 and 4 turbines staggered at initial 8*D* spacing (Fig. 9) shows different behaviour; it starts in a similar way to the other cases with the outer turbines moving outwards and the inner turbines moving downstream but then the inner turbines also start to move outwards producing a marked increase in array efficiency. The turbines move towards the edge of the wakes of the outer turbines until the wake model ceases to be valid (iteration 48). The experimental data indicate that the wake has little effect at

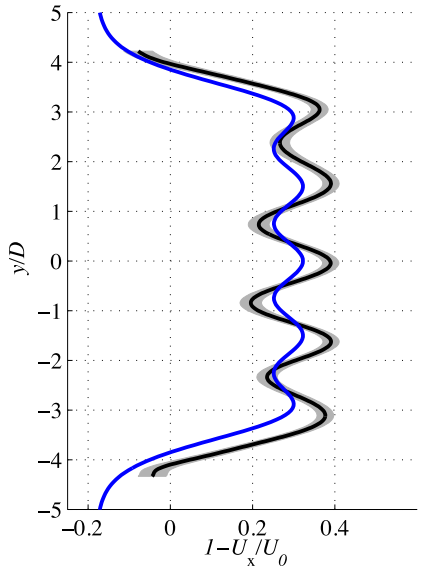

Fig. 3. Transverse velocity deficit at 12D downstream of front row for two rows of 5 turbines in in-line arrangement with 8D longitudinal spacing and 1.5D transverse spacing. Superposition model (blue), experiment (black with grey showing variation). (For interpretation of the references to color in this figure legend, the reader is referred to the web version of this article.)

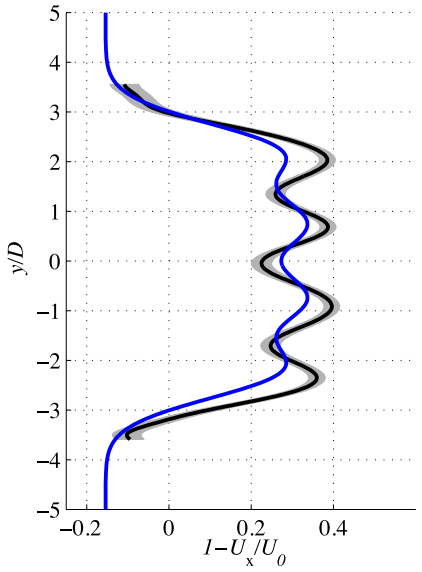

Fig. 5. Transverse velocity deficits at 12D downstream of front row for two rows of 3 and 4 turbines (upstream and downstream) in staggered arrangement with 8D longitudinal spacing and 1.5D transverse spacing. Superposition model (blue), experiment (black with grey showing variation). (For interpretation of the references to color in this figure legend, the reader is referred to the web version of this article.)

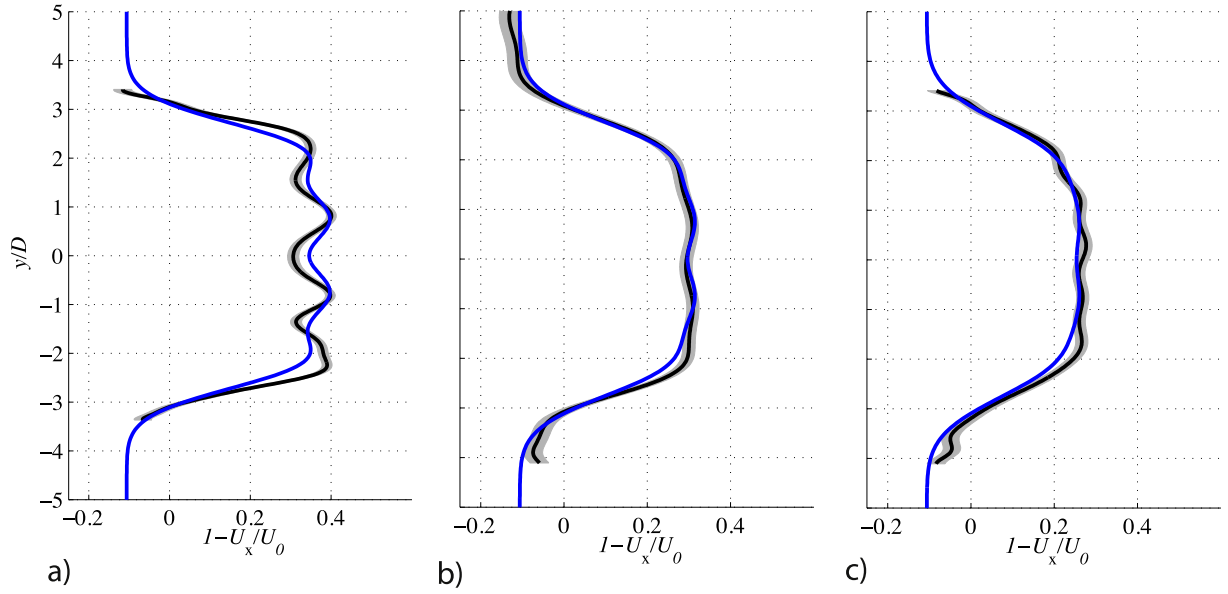

Fig. 4. Transverse velocity deficits at a) 8D, b) 10D and c) 12D downstream of front row for two rows of 3 and 4 turbines (upstream and downstream) in staggered arrangement with 4D longitudinal spacing and 1.5D transverse spacing. Superposition model (blue), experiment (black with grey showing variation). (For interpretation of the references to color in this figure legend, the reader is referred to the web version of this article.)

transverse distances greater than 1*D* from the centreline where the velocity is close to the ambient flow velocity (which in this case includes the velocity deficit from the upstream turbines). The array efficiency has increased by 24% to 0.96. The 3 row case with an initial spacing of 4*D* shown in Fig. 10 shows similar characteristics to the other two cases with the outer turbines moving outwards and the inner turbines downstream on both downstream rows. The array efficiency has increased by 36% to 0.79 with a maximum turbine movement of about 3*D*. The array efficiency was changing very slowly after 50 iterations (except for Fig. 9) and 55 was used for all cases.

Figs. 11–14 show the more important bi-directional flow results. It should be noted that the flow is quasi-steady and thus identical for a given flow direction when normalised by the onset flow velocity. This is thus not a time stepping problem but an iterative optimisation for successive flow directions and 5 iterations were used for a given flow direction (similar results were produced with 10). The two row case with an in line configuration turns out to be a special case. When flow reverses increased power would be obtained if downstream turbines were moved closer together, but this is considered impractical below 1.5*D*. This case with 5 turbines per row is converted to a staggered arrangement

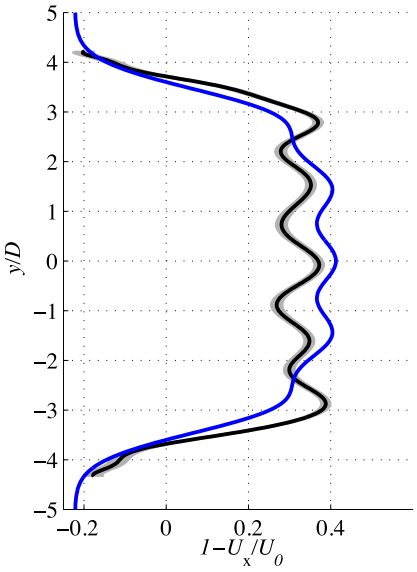

Fig. 6. Transverse velocity deficits at 12D downstream of front row for three rows of 3, 4 and 5 turbines (upstream to downstream) in staggered arrangement with 4D longitudinal spacing and 1.5D transverse spacing. Superposition model (blue), experiment (black with grey showing variation). (For interpretation of the references to color in this figure legend, the reader is referred to the web version of this article.)

array efficiency is dependent on maximum turbine movement and an array efficiency of 0.92 is obtained with a movement of about 3*D*. Similar characteristics are shown for the staggered configuration with rows of 3 and 4 turbines with longitudinal spacings of 4*D* (Fig. 12) and 8*D* (Fig. 13). For the former an array efficiency of 0.98 is achieved with a maximum movement of 2.8*D* and for the latter 0.97 with a maximum movement of 3.2*D*. For the 3 row case shown in Fig. 14 the characteristics are again similar with an array efficiency of 0.91 (an increase of 53%) from a maximum movement of 4*D*. However it can be seen that while overall array efficiency is generally increasing individual turbine efficiencies can decrease for the larger number of iterations within a certain flow direction while increasing at the change in flow direction. This occurs for the inner turbines in downstream rows and is due to small changes in position of one turbine affecting others, i.e. the optimisation for individual turbines has become cross coupled which is not accounted for, although the methodology for increasing net power clearly remains effective.

In all cases if the spacing were increased without restriction the array efficiency would become 100% but this is clearly not practically feasible and this approach enables net power increase to be assessed as a function of turbine spacing. The maximum number of turbines was 12 and this required about 20 min run time on a laptop. The code could easily be optimised to reduce this considerably and 100 or more turbines could readily be optimised.

Table 2
Velocity deficit errors in downstream traverses from superposition method.

Case	Distance downstream of upstream row	rms error in velocity deficit
1 (Fig. 1a–c)	4D, 8D, 10D	0.0193, 0.0224, 0.0333
2 (Fig. 2a–c)	4D, 8D, 10D	0.0609, 0.0233, 0.0260
3 (Fig. 3)	12D	0.0638
4 (Fig. 4a–c)	8D, 10D, 12D	0.0372, 0.0157, 0.0170
5 (Fig. 5)	12D	0.0601
6 (Fig. 6)	12D	0.0682

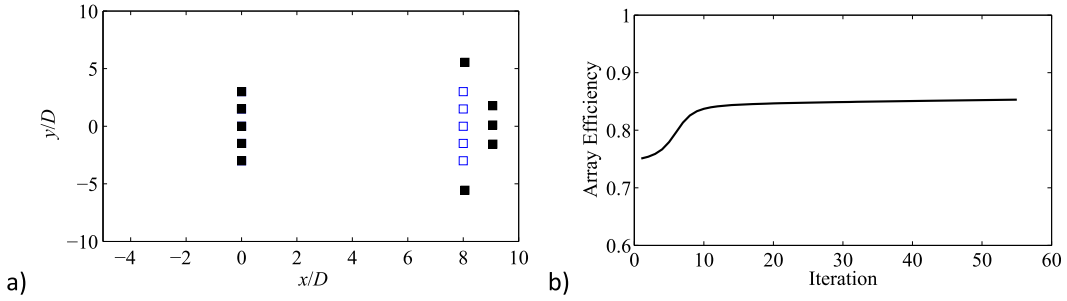

Fig. 7. (a) Initial (□) and final positions (■) after 55 iterations of two rows of 5 turbines in uni-directional flow with initial spacings of 8D longitudinal and 1.5D transverse; (b) Variation of array efficiency with iteration number, increased by 14%.

by displacing the second row transversely by ¾ *D* and results are shown in Fig. 11. It can be seen that turbines in both rows move predominantly transversely and array efficiency increases to over 0.92 after 50 iterations. It may be noted that there is a slight dip in net power at the point of flow reversal before it increases with further iterations. This is because the turbine configuration relative to flow direction is suddenly changed. Individual turbine efficiency is shown in Fig. 11c; this can be seen to be unity for upstream turbines and for downstream turbines increases for each flow direction as the iteration count increases giving a continuing increase in array efficiency. Finally Fig. 11d shows how

6. Discussion

In order to compare the method for wake prediction based on velocity deficit superposition with experimental velocity measurements (and thrust and power measurements) in a channel, blockage correction is clearly necessary. The basic method used here provides a uniform transverse blockage correction as in standard wind tunnel practice. With several turbines in a row the influence of local blockage can only be taken into account if the differential effect is known and it can be seen here that the simplest assumption of uniform blockage is quite effective. However

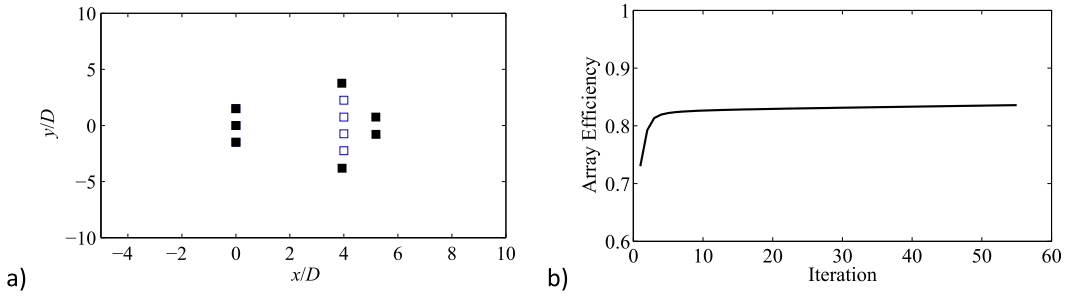

Fig. 8. (a) Initial (□) and final positions (■) after 55 iterations of two rows of 3 and 4 turbines in uni-directional flow with initial spacings of 4D longitudinal and 1.5D transverse; (b) Variation of array efficiency with iteration number, increased by 14%.

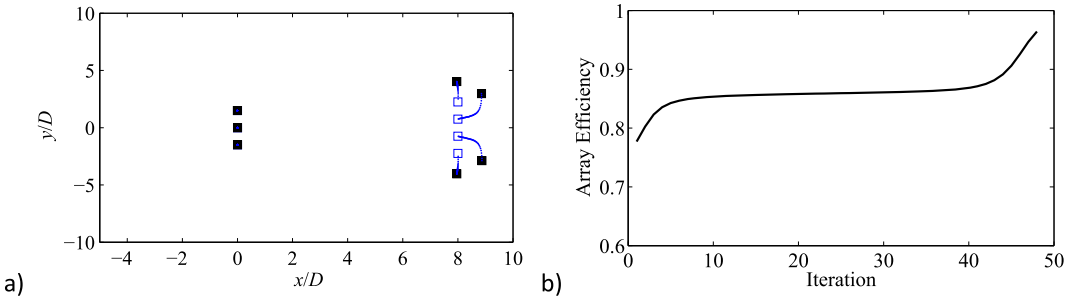

Fig. 9. (a) Initial (□) and final positions (■) after 48 iterations of two rows of 3 and 4 turbines in uni-directional flow with initial spacings of 8D longitudinal and 1.5D transverse; (b) Variation of array efficiency with iteration number, increased by 24%.

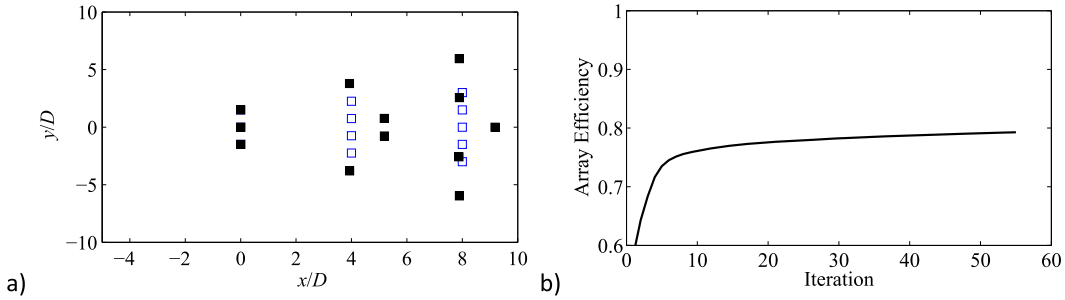

Fig. 10. (a) Initial (□) and final positions (■) after 55 iterations of three rows of 3, 4 and 5 turbines in uni-directional flow with initial spacings of 4D longitudinal and 1.5D transverse; (b) Variation of array efficiency with iteration number, increased by 36%.

accounting for variable blockage downstream is important and the parabolic formulation applied here (no upstream effect) is shown to be effective; to our knowledge this is quite novel.

These results are for idealised conditions at laboratory scale. In the field the flow direction will vary to some degree although this might be quite small during each ebb or flood tide [12]. The laboratory turbulence length scales and intensity are however likely to be representative with the ambient flow having length scales for longitudinal, transverse and vertical directions approximately in the ratio 5:3:1 [15] which are similar to field measurements [12] and the self-similar wake turbulence length scale is controlled by the wake width. While the method is appropriate for optimising power, only rotor wakes are considered here. In practice wakes of support structures should be taken into account. The self-similar rotor wake profile for a single turbine was for a depth/diameter, h/D, ratio of 1.67 and a diameter Reynolds number $Re = U_0 D/\nu$ of 1.3×10^5. This was well predicted with a RANS BEM model [10] and such a model may be used to give velocity deficit formulae for different h/D and Re values. As a steady flow this CFD model is the most efficient approach but time dependent models, such as actuator line or blade resolved RANS or LES models, could also be used, e.g. Ref. [1]. RANS BEM modelling has also been used for prediction of these array wake interactions [10] and this is in principle a more general approach than superposition, directly accounting for blockage. However for the cases investigated prediction accuracy was similar.

The superposition model has been shown to give good predictions of transverse wake width and velocity deficit for two or three rows of turbines. However with multiple rows individual wakes are likely to merge into a single large wake and different large scale structures are likely to develop, e.g. Ref. [2] for pile groups; superposition models (and RANS BEM models) will not pick up these effects which may include large scale unsteadiness from wake instability. A smoothly distributed drag representation in a shallow water model may reproduce these large scale wakes. A further problem is that depth-averaged shallow water models can grossly overestimate wake instability due to recirculating flows; this is because the effect of large horizontal turbulence length scales are not represented in causing bed shear which can be magnified by an order of magnitude in recirculating flows,

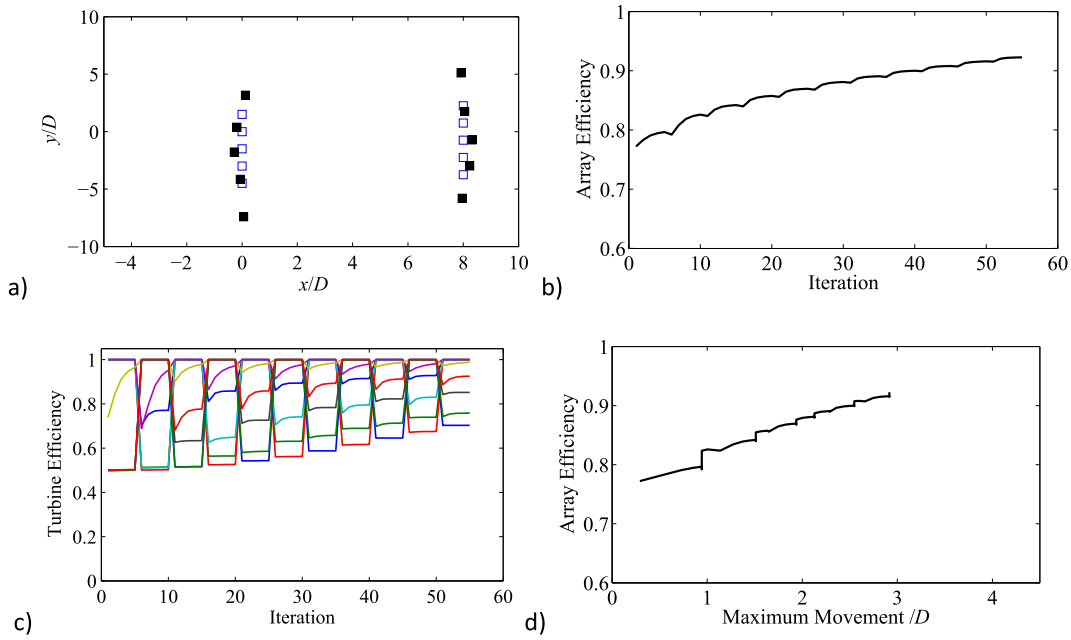

Fig. 11. (a) Initial (□) and final positions (■) after 55 iterations of two rows of 5 turbines in staggered arrangement in bi-directional flow with initial spacings of 8D longitudinal and 1.5D transverse; (b) Variation of array efficiency with iteration number, increased by 19%; (c) variation of individual turbine efficiency with iteration number; (d) variation of array efficiency with maximum turbine movement in units of diameter.

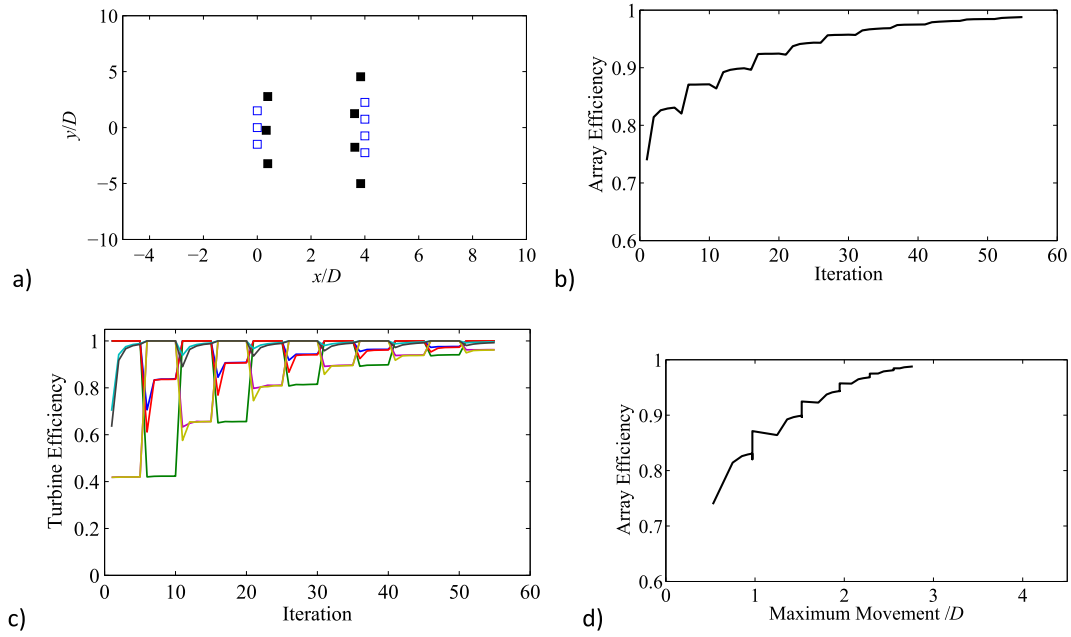

Fig. 12. (a) Initial (□) and final positions (■) after 55 iterations of two rows of 3 and 4 turbines in staggered arrangement in bi-directional flow with initial spacings of 4D longitudinal and 1.5D transverse; (b) Variation of array efficiency with iteration number, increased by 34%; (c) variation of individual turbine efficiency with iteration number; (d) variation of array efficiency with maximum turbine movement in units of diameter.

enhancing wake stability. This may be effectively predicted with a 3-D hydrostatic pressure model in which bed shear is implicit in the boundary layer calculation, not prescribed by a bed friction coefficient [17].

7. Conclusions

The method of velocity deficit superposition for turbine wake arrays has been shown to give good prediction of combined wake width and velocity deficits measured experimentally. The effect of blockage has to be estimated to compare with laboratory measurement and a method based on volume flux conservation has been developed accounting for variable downstream blockage. The superposition method is relatively simple and optimisation of turbine position for power generation is computationally very efficient. This has been applied to arrays with negligible blockage based on a chain rule formulation using the experimental configurations as initial conditions; array efficiencies of over 90% may be

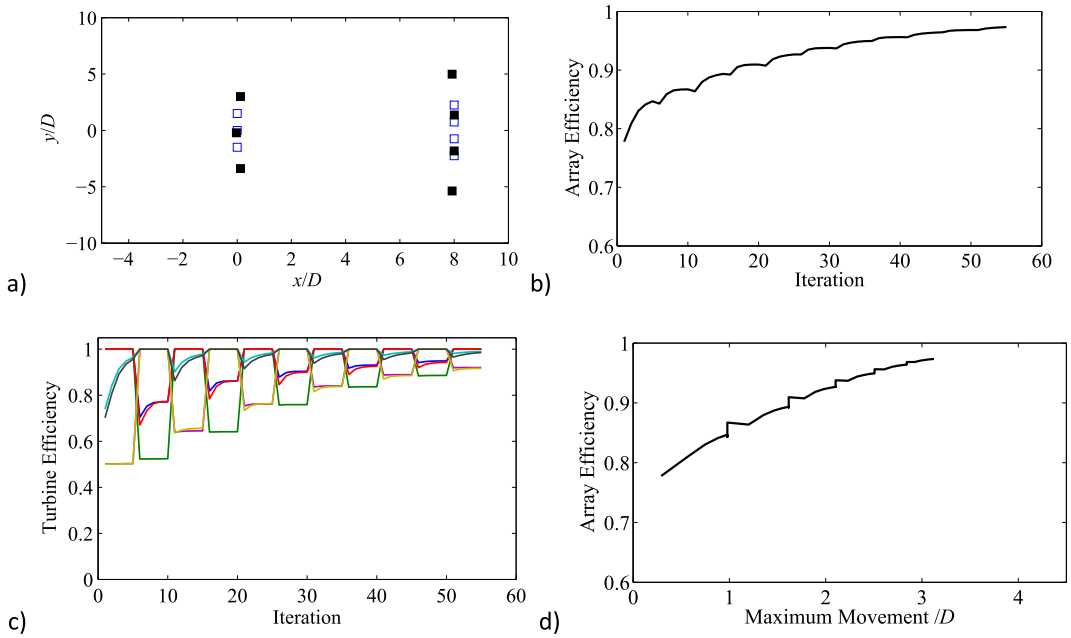

Fig. 13. (a) Initial (□) and final positions (■) after 55 iterations of two rows of 3 and 4 turbines in staggered arrangement in bi-directional flow with initial spacings of 8D longitudinal and 1.5D transverse; (b) Variation of array efficiency with iteration number, increased by 25%; (c) variation of individual turbine efficiency with iteration number; (d) variation of array efficiency with maximum turbine movement in units of diameter.

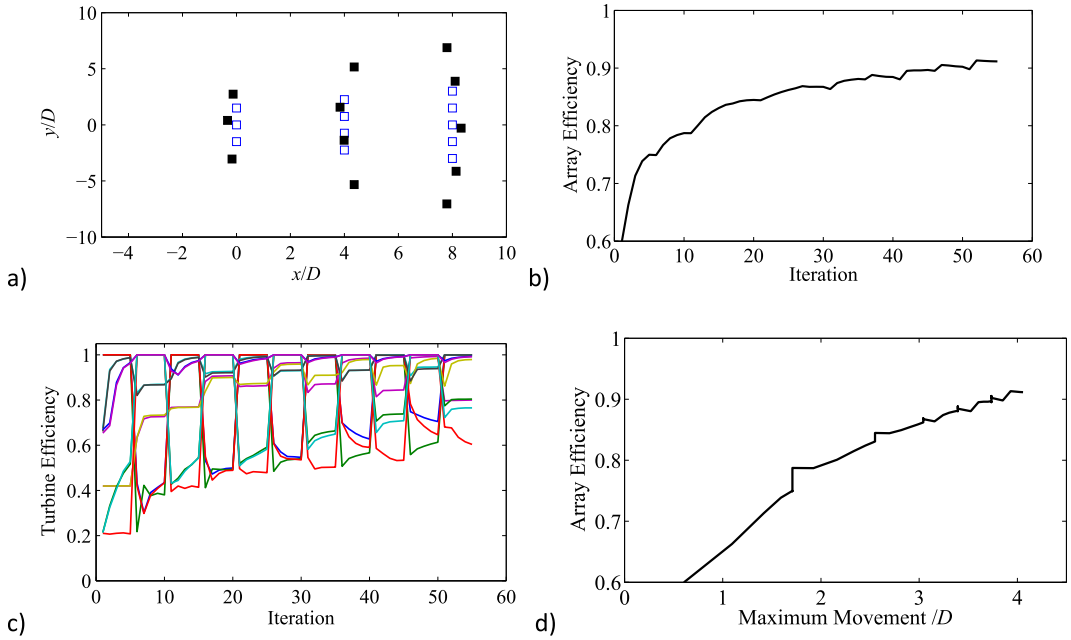

Fig. 14. (a) Initial (□) and final positions (■) after 55 iterations of three rows of 3, 4 and 5 turbines in staggered arrangement in bi-directional flow with initial spacings of 4D longitudinal and 1.5D transverse; (b) Variation of array efficiency with iteration number, increased by 53%; (c) variation of individual turbine efficiency with iteration number; (d) variation of array efficiency with maximum turbine movement in units of diameter.

achieved by movement of 3–4 diameters for bi-directional (oscillatory) flows. A rotor with different depth/diameter ratios and Reynolds number will have different self-similar velocity deficit profiles, required for superposition, which may be determined by CFD. The method has been shown to be reliable for two or three rows but may not capture large scale wake behaviour which would be generated by multiple rows. Nevertheless the method may be used to improve energy capture from some arrays with minimal extra deployment area.

Acknowledgements

The experimental equipment and part of the experimental database was developed as part of the Performance of Arrays of Wave and Tidal Array Systems (PerAWaT) project commissioned by the Energy Technologies Institute (ETI). Experiments were also conducted as part of the EPSRC grant EP/J010235/1 (X-MED) and through a PhD studentship funded by the United Kingdom Centre for Marine Energy Research EPSRC grant EP/I027912/1.

References

[1] U. Ahmed, I. Afgan, D.D. Apsley, T. Stallard, P.K. Stansby, CFD simulations of a full-scale tidal turbine: comparison of LES and RANS with field data, in: Proc. EWTEC 2015, Nantes, 2015.

[2] D.J. Ball, P.K. Stansby, N. Alliston, Modelling shallow-water low around pipe groups, Proc. Instn. Civ. Engrs. Wat. Marit. Energy 118 (1996) 226–236.

[3] T. Divett, R. Vennell, C. Stevens, Optimization of multiple turbine arrays in a channel with tidally reversing flow by numerical modelling with adaptive mesh, Phil. Trans. Roy. Soc. A371 (2013) 20120251.

[4] S. Draper, T. Stallard, P. Stansby, S. Way, T. Adcock, Laboratory scale experiments and preliminary modelling to investigate basin scale tidal stream energy extraction, in: Proc. EWTEC 2013, 890, Aalborg, 2013.

[5] S.W. Funke, P.E. Farrell, M.D. Piggott, Turbine array optimisation using the adjoint approch, Renew. Energy 63 (2014) 658–673.

[6] G.C. Larsen, From Solitary Wakes to Wind Farm Wind Fields a Simple Engineering Approach. Riso-R-1727(EN), Technical report, DTU Wind Energy, Roskilde, Denmark, 2009.

[7] E. Machefaux, G.C. Larsen, J.P. Murcia Leon, Engineering models for merging wakes in wind farm optimization applications, J. Phys. Conf. Ser. 625 (2015) 012037.

[8] R. Malki, I. Masters, A.J. Williams, T.N. Croft, Planning tidal stream turbine array layouts using a coupled blade element momentum - computational fluid dynamics model, Renew. Energy 63 (2014) 46–54.

[9] E. Maskell, A Theory of the Blockage Effects on Bluff Bodies and Stalled Wings in a Closed Wind Tunnel, Tech. Rep. 3400, Aeronautical Research Council Reports and Memoranda, 1965.

[10] A. Olczak, D. Sudall, T. Stallard, P.K. Stansby, Evaluation of RANS BEM and self-similar wake superposition for tidal stream turbine arrays. Proc. 11th European Wave and Tidal Energy Conference, EWTEC2015, Nantes, France, 7–10 Sep 2015.

[11] S.G. Parkinson, R. Willden, A. Wickham, T. Stallard, M. Thomson, Comparison of scale model wake data with an energy yield analysis tool for tidal turbine farms, in: Proc. 4th International Conference on Ocean Energy (ICOE). Dublin, 2012.

[12] B.G. Sellar, D. Sutherland, Tidal Energy Site Characterisation at the Fall of Warness, EMEC, UK, 2015. Energy Technologies Institute REDAPT report MA1001 MD3.8.

[13] S. Serhadloglu, T.A.A. Adcock, G.T. Houlsby, S. Draper, A.G.L. Borthwick, Tidal stream energy resource assessment of the Anglesey Skerries, Int. J. Mar. Energy 3 (2013) 98–111.

[14] T. Stallard, R. Collings, T. Feng, J. Whelan, Interactions between tidal turbine wakes: experimental study of a group of three-bladed rotors, Phil Trans. R. Soc. A Math. Phys. Eng. Sci. 371 (1985) (2013) 20120159.

[15] T.J. Stallard, T. Feng, P.K. Stansby, Experimental study of the mean wake of a tidal stream rotor in a shallow turbulent flow, J. Fluids Struct. 54 (2015) 235–246.

[16] P.K. Stansby, A. Slaouti, Simulation of vortex shedding including blockage by the random-vortex and other methods, Int. J. Numer. Methods Fluids 17 (1993) 1003–1013.

[17] P.K. Stansby, A mixing length model for shallow turbulent wakes, J. Fluid Mech. 495 (2003) 369–384.

[18] P.K. Stansby, Limitations of depth-averaged modelling of shallow wakes, ASCE J. Hydraul. Eng. 132 (7) (2006) 737–740.

[19] J.I. Whelan, T. Stallard, Arguments for modifying the geometry of a scale model rotor, in: 9th European Wave and Tidal Energy Conference (EWTEC). Southampton, UK, 2011.